Giant magnetostriction effect in LaFe12B6 metamagnet

L. V. B. Diop, J. Prokleška, O. Isnard

Giant magnetostriction effect in $LaFe_{12}B_6$ metamagnet

L.V.B. Diop[1†], J. Prokleška[2], O. Isnard[3]

[1]*Université de Lorraine, CNRS, IJL, F-54000 Nancy, France*

[2]*Charles University, Faculty of Mathematics and Physics, Department of Condensed Matter Physics, Ke Karlovu 5, Prague, Czech Republic*

[3]*Institut NEEL, Université Grenoble Alpes, CNRS, 25 rue des martyrs, F-38042 Grenoble, France*

We investigate the complex magnetic behavior of $LaFe_{12}B_6$ by means of magnetostriction, and thermal expansion measurements in applied fields of up to 14 T, elucidating the interplay between crystal lattice and spins. As main results, we have discovered a remarkably large negative thermal expansion (NTE) and giant magnetostriction in this itinerant-electron system. Of particular interest are the low-temperature magnetostriction isotherms ($T \leq 5$ K) all of which reach saturation discontinuously, by way of ultrasharp multistep transitions. These are rather unusual kind of first-order phase transitions. By contrast, the field-dependent magnetostriction varies smoothly at temperatures exceeding 5 K. A huge positive magnetostrictive effect of $\Delta V/V$ (20 K, 14 T) = 0.87% accompanies the field-induced first-order metamagnetic transition. In the vicinity of the Curie point, a magnetically driven giant NTE phenomenon with an average linear thermal expansion coefficient $\alpha_L = -27\times10^{-6}$ K^{-1} is observed.

Itinerant electron metamagnetic (IEM) transition, i.e., magnetic-field-induced first-order transition from a low-magnetized state to a high-magnetized state, is a very specific physical phenomenon that occurs in some rare earth–transition metal (R–T) intermetallics. It demonstrates technologically important multifunctionalities like prominent magnetoresistive, magnetostrictive, or magnetocaloric effects[1-4]. Metamagnets are a key component of the solid-state cooling technology (magnetic refrigeration) — an environmentally friendly promising alternative to conventional gas-compression/expansion refrigeration. In the past two decades, there has been a surge of interest in magnetic refrigeration due mainly to the discovery of giant magnetocaloric effect in the IEM system $La(Fe,Si)_{13}$[2]. This has triggered intense research of magnetic materials with first-order phase transitions. A good candidate to explore itinerant electron metamagnetism is $LaFe_{12}B_6$. The physics of this boride has been studied, revealing numerous intriguing features, anomalous magnetic behavior, and exotic physical properties. Indeed, discontinuous and uncommon avalanche-like metamagnetic transitions were observed

† leopold.diop@univ-lorraine.fr

in the magnetization process of $LaFe_{12}B_6$[5-8]. This unique and unconventional multistep behavior consists of a succession of abrupt magnetization jumps separated by plateaus giving rise to a staircase effect. Neutron diffraction experiments have shown that $LaFe_{12}B_6$ exhibits an amplitude-modulated magnetic structure. This antiferromagnetic spin arrangement is described by a wave vector $\mathbf{k}$ = (¼, ¼, ¼) and remarkably weak Fe magnetic moment (0.43 μ_B)[5]. Furthermore, $LaFe_{12}B_6$ is characterized by a particularly low ordering temperature T_N = 36 K for an Fe-rich compound, a critical point in the complex magnetic phase diagram with multiple step transitions[5], both conventional and inverse magnetocaloric effects[9], giant spontaneous magnetization jumps taking place after an incubation time in experimental conditions where both external parameters (temperature and applied magnetic field) are constant[7], and large hydrostatic pressure effects[10]. These powerful magnetoresponsive physical properties of relevance not only stimulated the development of new theoretical models and investigations under extreme conditions for a better understanding of the intriguing phenomenology of this alloy[10-14], but also highlight the potential interest of $LaFe_{12}B_6$ itinerant-electron metamagnet in future low-temperature energy technologies. The extreme sensitivity of its physical properties to either hydrostatic[10] or chemical[8,15,16] pressure makes $LaFe_{12}B_6$ an exceptional playground for condensed matter physics.

$LaFe_{12}B_6$ is the unique stable Fe-based member of the $RT_{12}B_6$ borides, whilst the $RCo_{12}B_6$ intermetallics are stable along the lanthanide series. Remarkable magnetotransport properties have been found in $RCo_{12}B_6$ (R = Y, Ho, and Gd)[17,18]. Contrary to the rather simple ferromagnetism of the isotype $LaCo_{12}B_6$ compound[19], $LaFe_{12}B_6$ displays more complex magnetic behavior as established by microscopic (neutron powder diffraction), and macroscopic (magnetization) measurements. Interestingly, $LaFe_{12}B_6$ is also the only compound within the $RT_{12}B_6$ (T = Co or Fe) family exhibiting an antiferromagnetic order with a Néel temperature much lower than the magnetic transition temperature of the $RCo_{12}B_6$ ferro- (R =Y, La-Sm) or ferri- (R = Gd-Tm) magnets (T_C =134 - 162 K)[19] and in any case an order of magnitude smaller when compared to the Curie point of any iron-rich R–Fe binary alloy. Hence, $LaFe_{12}B_6$ occupies a special place among R–Fe intermetallic compounds. Most recently, temperature- and magnetic-field-dependent x-ray diffraction studies performed on Ce-containing $La_{1-x}Ce_xFe_{12}B_6$ pseudo-ternary compounds have revealed a first-order structural phase transition associated with the antiferromagnetic-ferromagnetic (AFM-FM) and ferromagnetic-paramagnetic (FM-PM) transformations[20,21]. The field-induced lattice distortion converts the crystallographic structure from rhombohedral $R\bar{3}m$ (AFM, PM) to monoclinic *C2/m* (FM). This simultaneous magnetic-crystallographic transition is driven by magnetoelastic

coupling and is accompanied by giant negative magnetoresistance[20]. Unit-cell volume change as large as 0.9% is observed across the symmetry-lowering structural distortion (magnetostructural phase transition) in $La_{0.85}Ce_{0.15}Fe_{12}B_6$[20]. These findings prove the strong correlations between charge, spin, and lattice degrees of freedom in this Ce-doped alloy.

Although the magnetic and structural properties of the parent compound $LaFe_{12}B_6$ have been investigated in detail over the past decades, no works addressed the elastic properties of this boride. No studies have been reported on magnetostrictive effects. Our discovery of large magnetocaloric effects[9], which are due to the presence of magnetic-field-induced first-order AFM-FM and PM-FM metamagnetic transitions in $LaFe_{12}B_6$, prompted an investigation of the magnetovolume effects in this system. In this contribution, we present the elastic properties of $LaFe_{12}B_6$ model compound determined by linear thermal expansion, and magnetostriction experiments. We discuss the existence of huge magnetoelastic effects associated with the magnetic phase transitions in $LaFe_{12}B_6$ and thus making this ternary system a potential candidate as cryogenic magnetostrictive materials.

The intermetallic compound $LaFe_{12}B_6$ was synthetized by comelting appropriate amounts of pure components under Ar protective atmosphere in an arc melter. To ensure the sample homogeneity, the alloy was melted five times with the ingot being flipped over after each re-melting. The so-obtained button was wrapped in Ta foil, sealed in an evacuated quartz tube, followed by postannealing at 900 °C for 3 weeks. Details on the structural characterization of the $LaFe_{12}B_6$ polycrystalline sample are described in Ref. 5. The magnetostriction and linear thermal expansion (LTE) were measured using a high-resolution miniature capacitance cell dilatometer[22] connected to the Andeen-Hagerling 2500A capacitance bridge. The dilatometer was transferred into a Physical Property Measurement System (Quantum Design) cryostat for temperature and magnetic field control. For the experiments, a single specimen was cut in cubic shape (by wire saw) from the polycrystalline material. LTE measurements were carried out for zero-field cooled (ZFC) and field cooled (FC) protocols under various fields of up to 14 T. Length changes were measured along directions parallel ($\Delta L/L_{//}$) and perpendicular ($\Delta L/L_{\perp}$) to the applied field. From these isothermal magnetostriction data, the volume magnetostriction ($\Delta V/V = \Delta L/L_{//} + 2\Delta L/L_{\perp}$) and the anisotropic magnetostriction ($\Delta L/L_{//} - \Delta L/L_{\perp}$) were assessed. Temperature and field dependence of the magnetization was measured in a magnetic field of up to 14 T using a vibrating-sample magnetometer (Quantum Design PPMS-14).

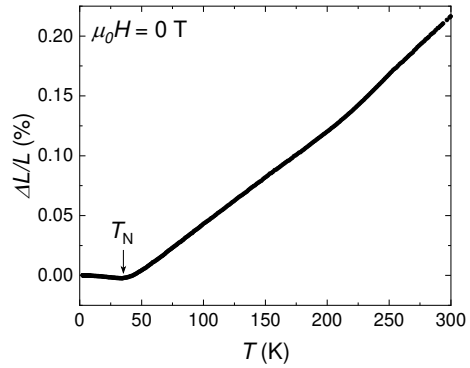

FIG. 1. Linear thermal expansion ($\Delta L/L$) as a function of temperature recorded in zero magnetic field for $LaFe_{12}B_6$.

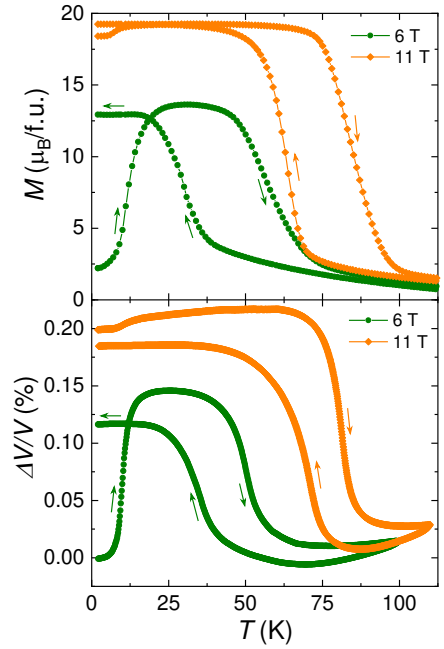

FIG. 2. Temperature dependence of the magnetization (top) and linear thermal expansion as a function of temperature of $LaFe_{12}B_6$ (bottom) measured in magnetic fields of 6 and 11 T.

The spontaneous ($\mu_0 H$ = 0 T) thermal expansion curve is displayed in Fig.1. Upon heating, $\Delta L/L$ continuously decreases down to the Néel temperature ≈ 34 K where it manifests an obvious change of curvature. This value is consistent with the AFM ordering temperature

derived from neutron powder diffraction and magnetization data[5,9]. In zero applied field, the thermal expansion increases as the temperature is lowered below T_N (negative thermal expansion, NTE). On the contrary, at elevated temperatures beyond T_N the material shrinks upon cooling (positive thermal expansion, PTE). No significant change in length was found at the Néel temperature, indicating weak magnetoelastic effects across the second-order AFM-PM magnetic phase transformation. The spontaneous ($\mu_0 H$ = 0 T) $\Delta L/L$ curve shows a change of slope at T^* = 210 K. This change of LTE coefficient in the paramagnetic state can be attributed to the temperature variation of the amplitude of spin fluctuations[31,32]. In itinerant-electron metamagnets, the amplitude of spin fluctuations increases upon heating and the thermal variation of spin fluctuations gives a positive contribution to the LTE coefficient in paramagnetic temperature ranges. This variation is mainly controlled by the longitudinal stiffness constant of spin fluctuations. The observed break (upturn) in the $\Delta L/L$ plot reflects the saturation of the local spin fluctuations of the 3*d* electrons at T^*.

Thermomagnetic curves *M(T)* recorded under various applied magnetic fields (6 and 11 T) are shown in Fig.2 (top panel). The 6 T ZFC *M(T)* curve exhibits a bell-like anomaly: upon heating, the system is partially converted into a FM state and then to the PM state. Cooling under 6 T leads to a magnetic phase transition from the PM state to a partially FM state. The results demonstrate that the magnetic transformation in $LaFe_{12}B_6$ depends on the direction of the temperature change. Furthermore, one can also observe that the maximum value of magnetization in the 6 T thermomagnetic curve is larger for the ZFC branch than for the FC leg. It is noteworthy that this last feature is rather unusual for standard ferromagnets in an applied field as large as 6 T. The isofield magnetization curve conducted in 11 T indicates that a big fraction, ~95%, of ZFC $LaFe_{12}B_6$ sample is transformed into FM phase at 2 K, and ~5% stays in the AFM ground state. The remaining proportion turns only at slightly higher temperature; giving rise to a small increase of magnetization on the low-temperature side of the 11 T ZFC curve.

The bottom panel of Fig. 2 illustrates the thermal dependence of the LTE of $LaFe_{12}B_6$ in ZFC and FC modes at different applied fields ($\mu_0 H$ = 6 and 11T). Upon heating in 11 T, $\Delta L/L$ initially increases and then shows a large drop of about 0.19% around 80 K in conjunction with the FM-PM magnetic transition. The disappearance of the ferromagnetic ordering results in a substantial lattice contraction, which is indicative of the occurrence of strong structural effects associated with the magnetic transition between the FM and PM states. During the cooling process ($\mu_0 H$ = 11 T), the material expands and then the length remains almost constant at

temperatures below ≈ 37 K. Another salient feature of the 11 T isofield LTE curve is the huge temperature hysteresis near the Curie point, which is one of the classical intrinsic signatures of a first-order phase transition.

Compared with the thermal behavior seen in zero and high magnetic fields, the $\Delta L/L$ curve recorded in 6 T differs considerably and displays an even more complex temperature dependence. Upon heating in $\mu_0 H$ = 6 T from the ground state at 2 K, the length variation of the thermally demagnetized $LaFe_{12}B_6$ compound exhibits a crossover from positive to negative thermal expansion, giving rise to a bell-shaped curve. This singular thermal evolution of $\Delta L/L$ is related to two magnetic events occurring sequentially upon heating. The first one is an order-order AFM→FM transition at low temperatures, and the second one corresponds to a FM to PM magnetic transformation at high temperatures. The steep increase in the linear thermal expansion by $\Delta L/L$ = 0.12%, when temperature is changed only by 5 K, denotes a sharp development of a high-magnetized state induced by temperature variation in a 6 T applied field. In other words, the onset of the FM order in $LaFe_{12}B_6$ is featured by a tremendous elongation. Upon cooling in 6 T, the lattice undergoes an expansion, followed by a saturation of $\Delta L/L$ in the low-temperature regime. As it can be clearly observed in Fig. 2, the 6 T forced magnetostriction plot presents a strong divergence and a remarkably large thermal hysteresis of ~18 K between the ZFC and FC data.

The thermal evolution of $\Delta L/L$ manifests magnetic events that are very much similar to the ones evidenced in the temperature-dependent magnetization curves. This obviously demonstrates the consistency in the magnetization and magnetostriction data. As follows from Fig. 2, the magnetic ordering temperature is strongly shifted toward higher temperatures upon increasing the strength of the external field. In $LaFe_{12}B_6$ the applied field favors tendencies to FM state. A pronounced NTE phenomenon is found in the 6 T ZFC curve over a wide temperature window of ΔT~50 K leading to an average linear thermal expansion coefficient $\alpha_L = (1/L)(\Delta L/\Delta T) = -27\times10^{-6}$ K^{-1}. This prominent NTE effect ensues from the strong coupling between the crystal and magnetic sublattices. The NTE coefficient obtained here for $LaFe_{12}B_6$ is comparable with the value reported for $LaFe_{10.5}CoSi_{1.5}$[23] metamagnet, $\alpha_L = -26\times10^{-6}$ K^{-1}. In terms of absolute value, α_L of $LaFe_{12}B_6$ intermetallic compound is 3 times higher than that of the currently used commercial NTE material ZrW_2O_8[24] ($\alpha_L = -9\times10^{-6}$ K^{-1}).

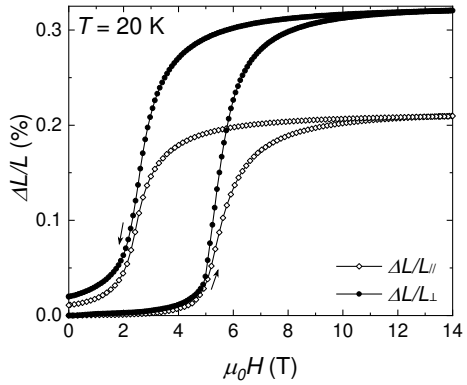

FIG. 3. Parallel ($\Delta L/L_{//}$) and perpendicular ($\Delta L/L_{\perp}$) magnetostriction isotherms recorded at 20 K for $LaFe_{12}B_6$.

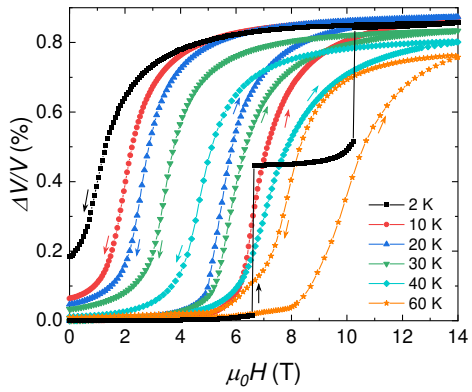

FIG. 4. Volume magnetostriction isotherms of $LaFe_{12}B_6$ measured between 2 and 60 K.

To further examine the volume change due to the IEM transition, the longitudinal ($\Delta L/L_{//}$) and transverse ($\Delta L/L_{\perp}$) magnetostrictions were measured at some selected temperatures. For this study, the system was first thermally demagnetized in the paramagnetic regime and then zero-field cooled down to the measurement temperature. For each isothermal magnetostriction curve, the applied field was cycled between 0 and 14 T. The corresponding results for T = 20 K are depicted in Fig. 3. At 20 K in the AFM state, the value of $\Delta L/L_{//}$ is practically negligible below ≈ 4.5 T; however, it increases rapidly as the intermetallic compound endures a metamagnetic transition. Like the magnetization isotherm[5], $\Delta L/L_{//}$ displays hysteretic behavior, characteristic of a first-order transition. The transverse magnetostriction,

$\Delta L/L_{\perp}$, also experiences a very fast rise during the metamagnetic process. The magnitude of $\Delta L/L_{\perp}$ is much higher than that of $\Delta L/L_{//}$ at the maximum attainable field 14 T ($\Delta L/L_{//}$ = 0.21% and $\Delta L/L_{\perp}$ is = 0.33% at 20 K). This indicates an anisotropic expansion with a more pronounced change in dimension along the direction perpendicular to the applied magnetic field. The anisotropic magnetostriction amounts to -0.11% at 20 K and 14 T.

We exemplify in Fig. 4 the isothermal volume magnetostriction plots at various temperatures in the AFM and PM regions. During the first increase of the applied field at 2 K, step-like changes of the material dimensions are detected at characteristic fields. The 2 K virgin magnetostriction curve shows two abrupt discrete jumps at $\mu_0 H_{cr1}$ = 6.65 T and $\mu_0 H_{cr2}$ = 10.25 T. During the first jump $\Delta V/V$ suddenly increases from 0.015% to 0.45%. At the second ultrasharp step it evolves from 0.51% to 0.84%. The final deformation state at 14 T corresponds to the fully FM polarized phase. These unusual step-like changes are interpreted as resulting from conversion of a fraction of the sample from the AFM state into the FM state. The intermediate volume plateau following the first jump corresponds to a mixture of the initial AFM and field-induced FM phases, i.e., a magnetically heterogeneous state (mixed phase AFM + FM or phase separated into AFM and FM domains). No discontinuity is observed in the subsequent reverse leg and the initial value of the volume is not recovered after reducing the external field to zero. This feature supports the conclusion that the field-induced AFM-FM phase transformation is partially reversible in the temperature range below T_N[9]. To restore the initial volume value of the virgin state (AFM ground state), $LaFe_{12}B_6$ alloy should be warmed up above the Curie point and then cooled down in the absence of an external magnetic field.

At temperatures above 5 K, the nature of the volume magnetostriction isotherms changes drastically. $\Delta V/V$ varies progressively across both AFM-FM and PM-FM metamagnetic transitions in contrast to the discontinuous behavior observed at 2 K. The isothermal magnetostriction plots show large magnetic field hysteresis, bearing witness to the first-order character of the transition. The hysteresis width is estimated to be 4.9 T at 10 K and diminishes upon increasing temperature. The critical magnetic field of the downward-field path of the metamagnetic transformation decreases continuously upon cooling. However, the thermal variation of the transition field obtained for the ascending-field scan is nonmonotonic. Below 20 K the critical field of the first-order AFM-FM phase transition increases with lowering the temperature while it shows the opposite trend at higher temperatures. Below 20 K, the transition field rises upon cooling due to the enhancement of the negative exchange interactions and the diminution of the thermal fluctuations of the magnetic moments and/or

elasticity of the lattice in the AFM ground state[8,21,28]. This results in the increase of both the free energy difference between the AFM and FM states, and the critical magnetic field required to accomplish the transition from one state to another. Under isothermal conditions, the application of a magnetic field at or above the critical transition field is necessary to overcome the energy barrier between magnetic phases.

The relative change in volume due to the field-induced metamagnetic transition reaches a value of $\Delta V/V$ (20 K, 14 T) = 0.87%. This value of the forced volume magnetostriction obtained here for $LaFe_{12}B_6$ compares very well with the unit-cell volume change of 0.9% due to the symmetry breaking transition unveiled by in-field x-ray powder diffraction investigations undertaken on Ce-containing $La_{0.85}Ce_{0.15}Fe_{12}B_6$[20] pseudo-ternary alloy. It should be noted that $\Delta V/V$ in $LaFe_{12}B_6$ is also comparable in magnitude to the isotropic volume variation associated with the IEM transformation in Fe-rich intermetallics like $La(Fe_xAl_{1-x})_{13}$ and $La(Fe_xSi_{1-x})_{13}$. Indeed, relative volume changes of 1% and 0.9% were reported for $La(Fe_{0.87}Al_{0.13})_{13}$[25] and $La(Fe_{0.86}Si_{0.14})_{13}$[26], respectively.

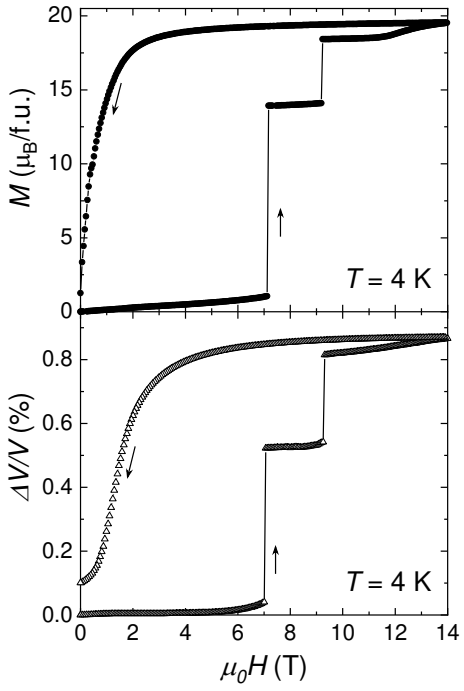

FIG. 5. Magnetization (top) and magnetostriction (bottom) isotherms of $LaFe_{12}B_6$ at 4 K.

In Fig. 5 we present both the magnetization and the magnetostriction of $LaFe_{12}B_6$ as a function of applied field at 4 K. The isothermal magnetostriction curve exhibits sharp stepwise changes in the same magnetic field intervals where steep discontinuities are observed in the magnetization isotherm. It is quite evident that these anomalous features are not merely magnetic in origin, yet they have a contribution from the strong spin-lattice coupling. The avalanche-like transition phenomena can be attributed to the field-induced crystallographic distortion which is driven by magnetoelastic coupling in the $RFe_{12}B_6$ family[20,21]. In this intermetallic system, the forced FM state is a structurally distorted phase. Elastic strains develop at the AFM/FM interfaces due to the difference in crystal lattice between the two magnetically ordered phases. Upon applying suitable magnetic field, FM domains are likely to grow inside the AFM matrix but the interfacial constraints act against this to stop the development of the FM regions[20,29]. The driving force acting on the spins increases as the external applied field is continuously raised. When the magnetic force is strong enough to overcome the elastic strain energy, the FM phase grows catastrophically, resulting in sudden jumps in magnetostriction and magnetization. These extremely sharp steps reflect a burst-like growth of the FM component within the AFM matrix. The transformation evolves by a succession of jumps between metastable states[30] and this affect all the related physical properties.

The large thermal and magnetic field hysteresis of the LTE and isothermal magnetostriction curves are remarkable features and in harmony with the hysteretic behavior observed in the macroscopic magnetic data. The abrupt magnetostriction jumps are impressively similar to the ultrasharp magnetization steps. Overall, the forced volume magnetostriction isotherms qualitatively resemble the isothermal magnetization curves; illustrating the strength of the coupling between magnetism and crystal lattice in $LaFe_{12}B_6$. This most likely arises from the extreme sensitivity of the exchange interactions between Fe atoms to the interatomic distances[27]. Our data on thermal expansion and magnetostriction undoubtedly prove that giant magnetovolume effects accompany the first-order metamagnetic transition. The external field triggers a magnetic phase transformation from a low-volume low-magnetized state to a high-volume high-magnetized state. These experimental findings point to the relative magnetic phase stability and demonstrate that $LaFe_{12}B_6$ manifests competition between AFM and FM exchange interactions. $LaFe_{12}B_6$ is a system where the highly itinerant Fe magnetism is poised on the verge of ferromagnetic order. In itinerant-electron systems, the volume magnetostriction arises in order to reduce the kinetic energy of 3*d* electrons increased by the exchange split of 3*d* band[25]. Consequently, the volume magnetostriction is correlated to the mean-square amplitude of the local magnetic moment.

To summarize, we have observed giant magnetoelastic effects across the temperature- and field-induced first-order AFM-FM and PM-FM phase transitions in $LaFe_{12}B_6$. The thermal expansion and magnetostriction data revealed multiple prominent features including a crossover from PTE to NTE phenomenon, a huge temperature hysteresis, steep jumps, and a strong field hysteresis. A remarkably large magnetostrictive effect of 0.87% has been obtained, making $LaFe_{12}B_6$ itinerant-electron metamagnet a potential candidate as cryogenic magnetostrictive materials. However, the magnetic transitions occur at relatively high critical fields with large hysteresis, and these are limitations for technical applications of this boride in a high performance cryogenic magnetostrictive actuator.

Further investigations such as elastic moduli measurements on single crystals are required in the future and may provide more extended information.

AUTHOR DECLARATIONS

Conflict of Interest

The authors have no conflicts to disclose.

Author Contributions

L.V.B. Diop: Resources (lead); Conceptualization (lead); Formal Analysis (lead); Visualization (lead); Project Administration (equal); Writing-Original Draft Preparation (lead); Writing – review and editing (equal). **J. Prokleška**: Data curation (lead); Resources (supporting); Writing-Original Draft Preparation (supporting). **O. Isnard**: Resources (supporting); Project Administration (equal); Writing – review and editing (equal).

DATA AVAILABILITY

The data that support the findings of this study are available from the corresponding author upon reasonable request.

REFERENCES

[1]D.P. Kozlenko, E. Burzo, P. Vlaic, S.E. Kichanov, A.V. Rutkauskas, and B.N. Savenko, Sci. Rep. **5**, 8620 (2015).

[2]A. Fujita, S. Fujieda, Y. Hasegawa, and K. Fukamichi, Phys. Rev. B **67**, 104416 (2003).

[3]H. Yamada, and T. Goto Phys. Rev. B **68**, 184417 (2003).

[4]N.H. Duc, D.T. Kim Anh, and P.E. Brommer, Physica B **319**, 1 (2002).

[5]L.V.B. Diop, O. Isnard, and J. Rodríguez-Carvajal, Phys. Rev. B **93**, 014440 (2016).

[6]S. Fujieda, K. Fukamichi, and S. Suzuki, J. Magn. Magn. Mater. **421**, 403 (2017).

[7]L.V.B. Diop, and O. Isnard, Appl. Phys. Lett. **108**, 132401 (2016).

[8]L.V.B. Diop, and O. Isnard, Phys. Rev. B **97**, 014436 (2018).

[9]L.V.B. Diop, and O. Isnard, J. Appl. Phys. **119**, 213904 (2016).

[10]L.V.B. Diop, O. Isnard, Z. Arnold, J.P. Itié, J. Kastil, and J. Kamarad, Solid State Comm. **252**, 29 (2017).

[11]G.I. Miletic, and Z. Blazina, J. Magn. Magn. Mater. **323**, 2340 (2011).

[12]G.I. Miletic, and Z. Blazina, J. Alloys Compd. **430**, 9 (2007).

[13]M. Rosenberg, T. Sinnemann, M. Mittag, and K.H.J. Buschow, J. Alloys Compd. **182**, 145 (1992).

[14]Q.A. Li, C.H. de Groot, F.R. de Boer, and K.H.J. Buschow, J. Alloys Compd. **256**, 82 (1997).

[15]X. Chen, Y. Mudryk, A.K. Pathak, and V.K. Pecharsky, J. Alloys Compd. **884**, 161115 (2021).

[16]Z. Ma, X. Dong, Z. Zhang, and L. Li, J. Mater. Sci. Technol. **92**, 138 (2021).

[17]F. Mesquita, S.G. Magalhaes, P. Pureur, L.V.B. Diop, and O. Isnard, Phys. Rev. B **101**, 224414 (2020).

[18]F. Mesquita, L. V. B. Diop, G. Fraga, O. Isnard, and P. Pureur, IEEE Mag. Lett. **6**, 1 (2015).

[19]M. Mittag, M. Rosenberg, and K.H.J. Buschow, J. Magn. Magn. Mater. **82**, 109 (1989).

[20]L.V.B. Diop, T. Faske, O. Isnard, and W. Donner, Phys. Rev. Mater. **5**, 104401 (2021).

[21]L.V.B. Diop, T. Faske, M. Amara, D. Koch, O. Isnard, and W. Donner, Phys. Rev. B **104**, 134412 (2021).

[22]M. Rotter, H. Müller, E. Gratz, M. Doerr, and M. Loewenhaupt, Rev. Sci. Instrum. **69**, 2742 (1998).

[23]R. Huang, Y. Liu, W. Fan, J. Tan, F. Xiao, L. Qian, and L. Li, J. Am. Chem. Soc. **135**, 11469 (2013).

[24]A.W. Sleight, Inorg. Chem. **37**, 2854 (1998).

[25]K. Irisawa, A. Fujita, K. Fukamichi, M. Yamada, H. Mitamura, T. Goto, and K. Koyama, Phys. Rev. B **70**, 214405 (2004).

[26]A. Fujita, Y. Akamatsu, and K. Fukamichi, J. Appl. Phys. **85**, 4756 (1999).

[27]L. Néel Ann. Phys. **5**, 232 (1936).

[28]E. M. Levin, K. A. Gschneidner, Jr., and V. K. Pecharsky, Phys. Rev. B **65**, 214427 (2002).

[29]B. Maji, K. G. Suresh, and A. K. Nigam, Europhys. Lett. **91**, 37007 (2010).

[30]V. Hardy, S. Hebert, A. Maignan, C. Martin, M. Hervieu, and B. Raveau, J. Magn. Magn. Mater. **264**, 183 (2003).

[31]Y. Takahashi, *Spin fluctuation theory of itinerant electron magnetism* (Springer-Verlag, Heidelberg, 2013).

[32]T. Moriya, and K. Usami, Solid State Commun. **34**, 95 (1980).

PLEASE CITE THIS ARTICLE AS DOI: 10.1063/5.0144348

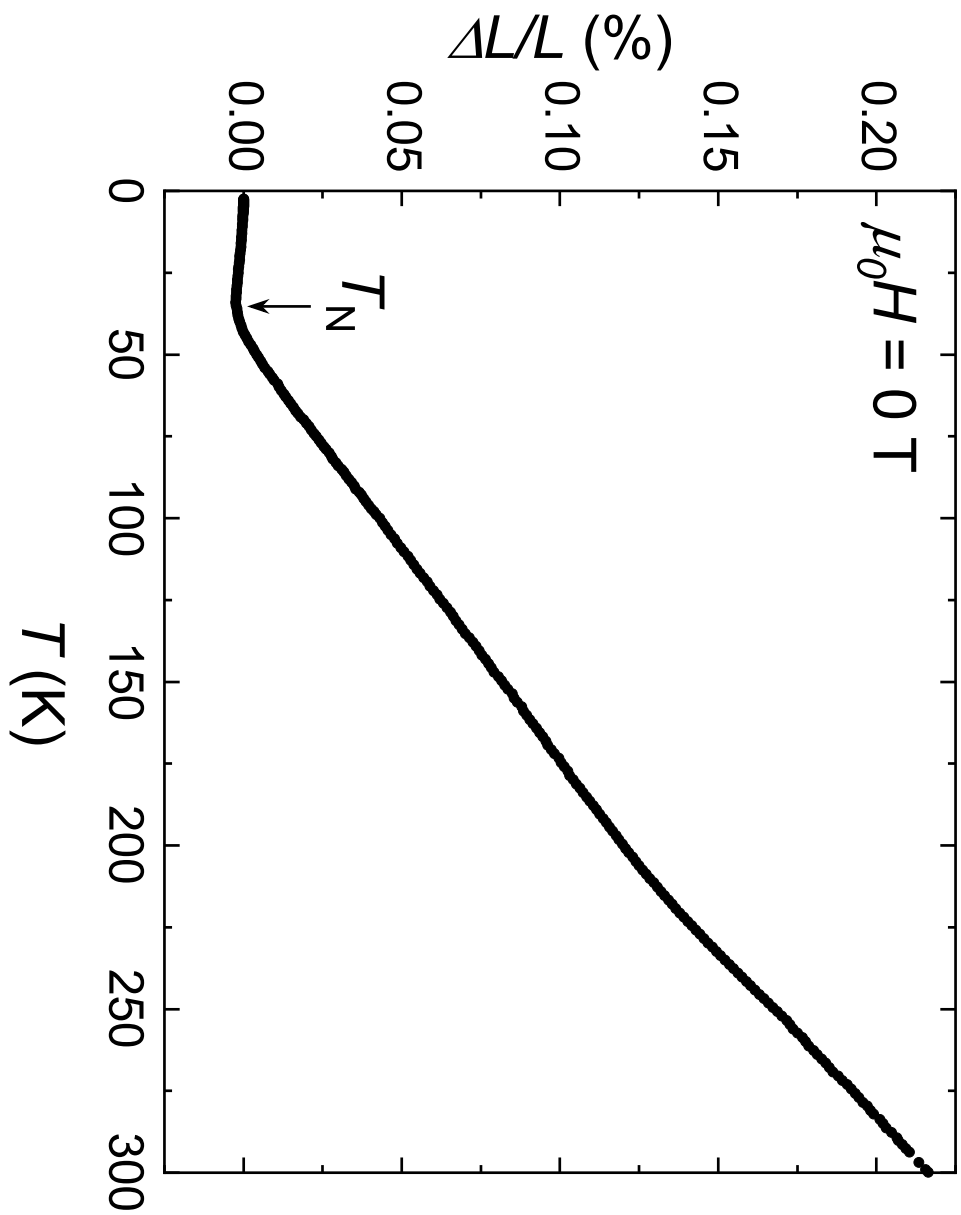

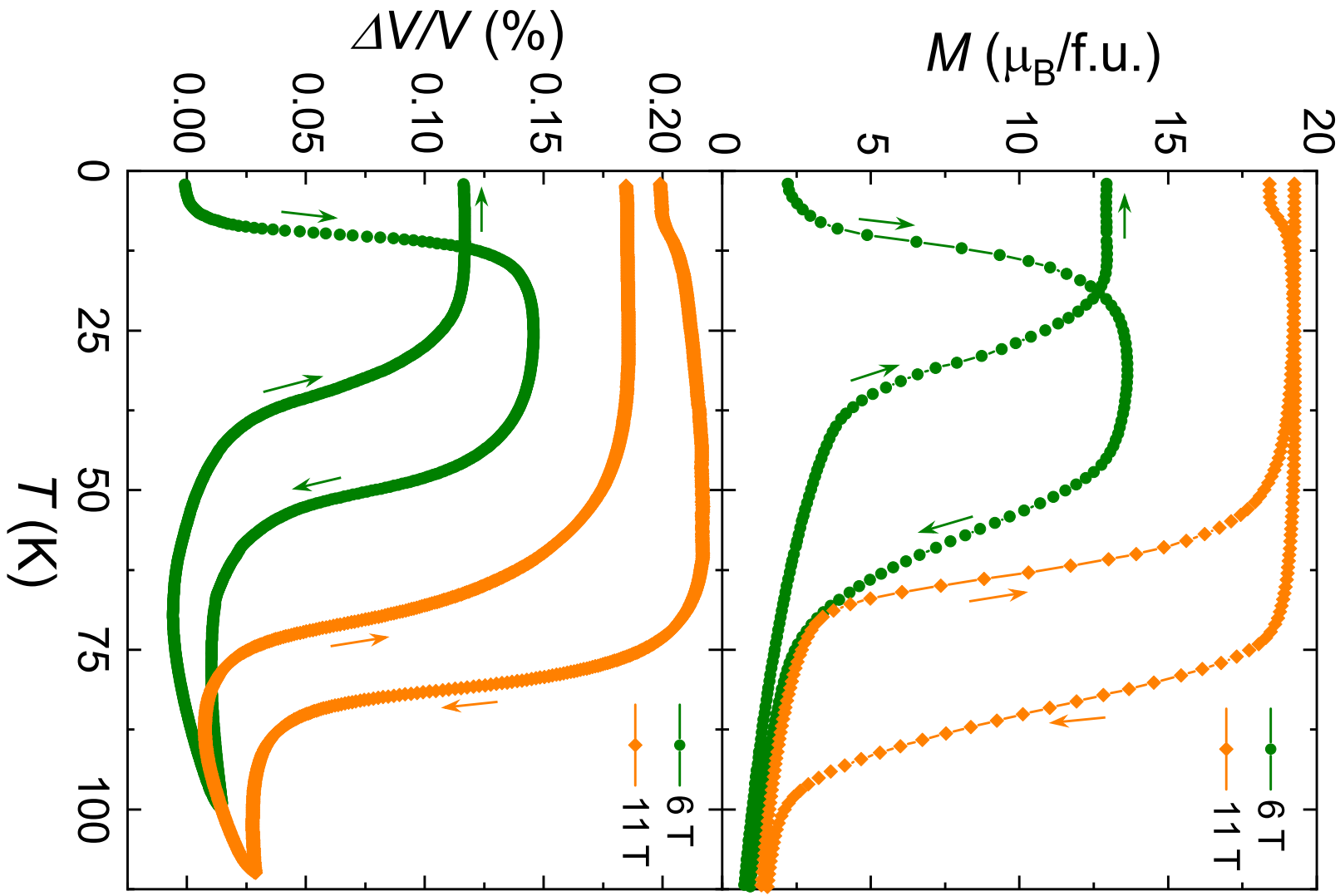

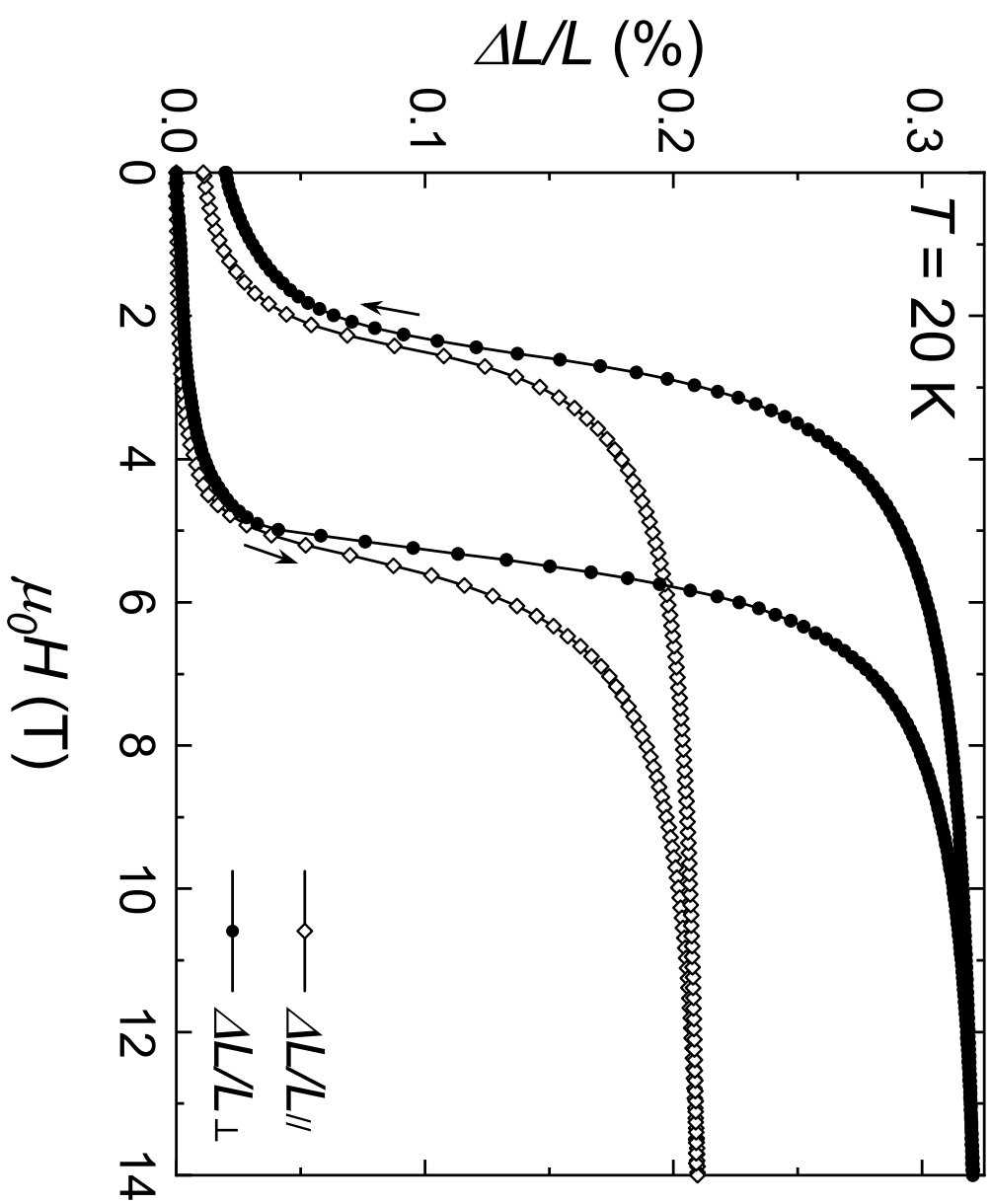

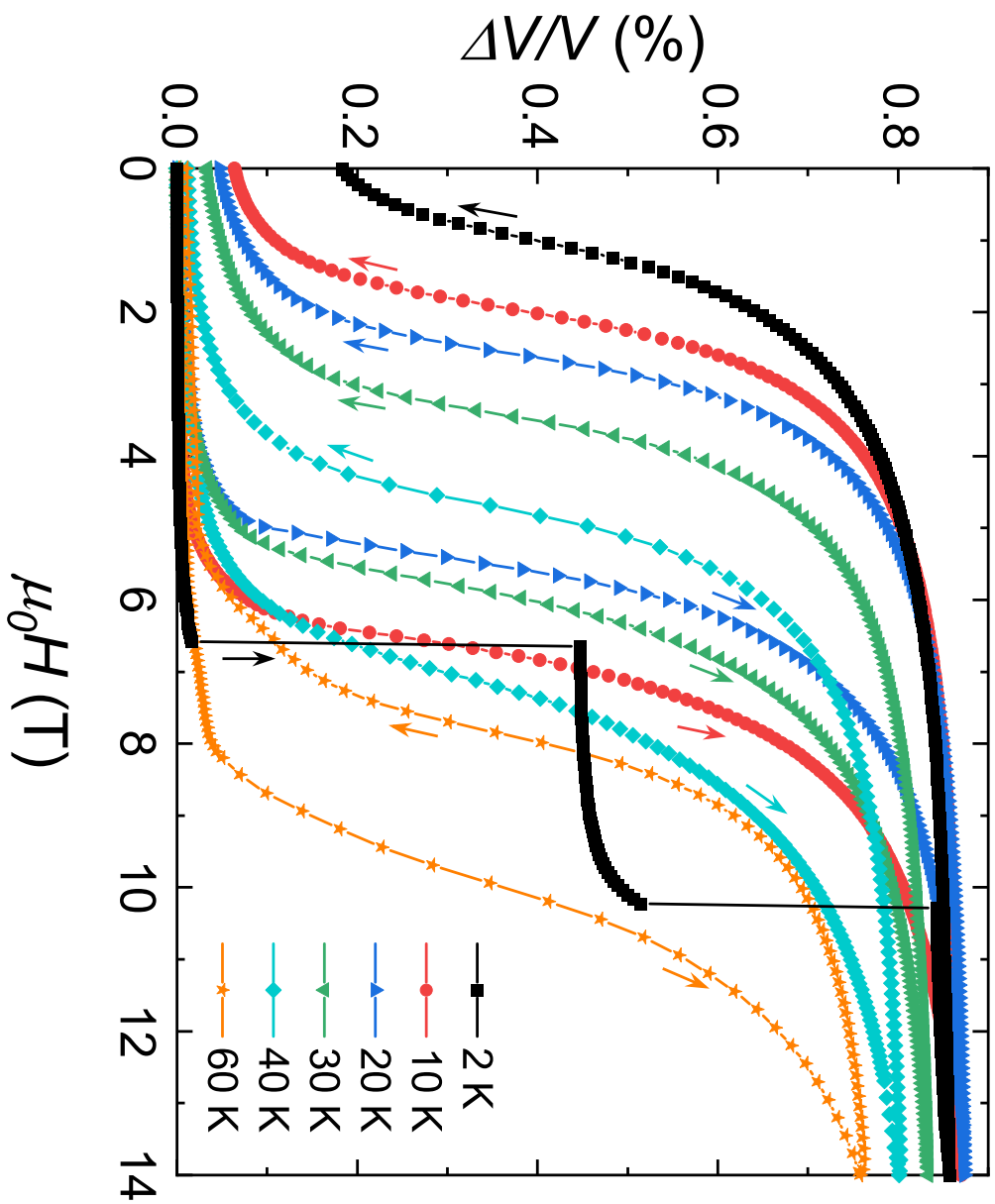

PLEASE CITE THIS ARTICLE AS DOI: 10.1063/5.0144348